

Surface plasmon Fourier optics

A. Archambault, T. V. Teperik,^{*} F. Marquier, and J. J. Greffet[†]

Laboratoire Charles Fabry, Institut d'Optique, CNRS, Université Paris-Sud, Campus Polytechnique, RD 128, 91127 Palaiseau Cedex, France

(Received 17 February 2009; revised manuscript received 17 April 2009; published 13 May 2009)

Surface plasmons are usually described as surface waves with either a complex wave vector or a complex frequency. When discussing their merits in terms of field confinement or enhancement of the local density of states, controversies have arisen as the results depend on the choice of a complex wave vector or a complex frequency. In particular, the shape of the dispersion curves depends on this choice. In this work, we derive two equivalent vectorial representations of a surface plasmon field using an expansion over surface waves with either a complex wave vector or a complex frequency. These representations can be used to discuss the issue of field confinement and local density of states as they have a nonambiguous relation with the two dispersion relations. They can also be used to account for propagation and diffraction of surface waves. They generalize the scalar approximation often used when discussing surface plasmon diffraction.

DOI: [10.1103/PhysRevB.79.195414](https://doi.org/10.1103/PhysRevB.79.195414)

PACS number(s): 73.20.Mf, 42.30.Kq, 78.20.Bh

I. INTRODUCTION

Surface plasmons have been known since the pioneering work of Ritchie¹ in the 1950s. Considerable advances made in nanotechnology in recent years and the desire to control and manipulate light at nanoscale have renewed the interest in surface plasmons.² Numerical simulations and experiments have demonstrated unique properties of different plasmonic nanostructures such as extraordinary transmission,^{3,4} guiding,^{5–8} fluorescence enhancement,^{9–13} field enhancement,^{14–16} focusing,¹⁷ super-resolution,^{18–20} omnidirectional absorption,^{21,22} and coherent thermal emission.^{22–24}

In this paper, we shall focus on surface plasmons propagating along flat surfaces. Propagation of surface plasmons on a flat surface perpendicular to the z axis is often discussed using a mode whose electric field $\mathbf{E}(z)\exp[i(K_x x + K_y y - \omega t)]$ is characterized by a frequency ω and a wave vector $\mathbf{K} = K_x \hat{x} + K_y \hat{y}$ parallel to the interface. However, the surface plasmon fields diffracted by edges, guided by ridges, or focused by lenses cannot be described by a simple mode. It is well known that a finite-size beam propagating in a vacuum has to be described in terms of a linear superposition of plane waves. To address the corresponding issue for surface plasmons, different ansatz,^{5,25,26} often neglecting polarization, have been used in the literature. One of the goals of this paper is to derive a rigorous representation for the surface plasmon field. Such a superposition is the equivalent of the angular plane-wave spectrum for surface plasmons. It can be used to develop a framework for surface plasmon Fourier optics.

In doing so, difficulty arises. When losses are taken into account, a mode with real \mathbf{K} and real ω is no longer a valid solution. Although we can still use a Fourier representation with real \mathbf{K} and real ω , it is not convenient to deal with waves that are not a solution of Maxwell equations for the interface problem. Elementary solutions using either a complex \mathbf{K} or a complex ω can be found. However, we cannot assume that they form a basis. The first issue is thus to derive a general representation for the surface plasmon field as a superposition of modes. The second issue is related to the dispersion relation.

A dispersion relation can be found when using either a complex \mathbf{K} and a real ω or vice versa. These two choices lead to different shapes as seen in Fig. 1. One dispersion relation has an asymptote for very large values of K while the other has limited values of K and presents a backbending. This issue was first noted by Arakawa *et al.*²⁷ and later discussed by Alexander *et al.*²⁸ Arakawa²⁷ remarked that when plotting the position of the dips in a reflectivity experiment where the angle of incidence is varied at fixed frequency, one finds the dispersion relation with backbending. Instead, when plotting the points obtained from a spectrum at fixed angle, one finds the dispersion relation without backbending. This approach seems simple and easily applicable. It is sufficient to explain the attenuated total reflection (ATR) experiments. Nevertheless, it is not a general prescription that can be used to discuss all possible issues. Let us illustrate this point by addressing two questions regarding the most important properties of surface plasmons: confinement of the fields and large density of states (DOS). For a theoretical discussion of these applications, different dispersion relations lead to different predictions. Confinement of the field is the key property regarding applications such as optical lithography, enhanced nonlinear effects, or super-resolution issues. The dispersion relation with a backbending predicts a cut-off spatial frequency and therefore a resolution limit, whereas the dispersion relation without backbending does not predict any resolution limit. Enhancement of the local density of states (LDOS) (or Purcell effect) is fundamental for fluorescence enhancement and more light emission assisted by surface plasmons. The dispersion relation with a backbending again predicts a cut-off spatial frequency and therefore an upper limit to the LDOS. No limit is predicted by the other dispersion relation. A general discussion on the applicability of the different dispersion relations is thus needed.

In this paper we start by deriving two general representations of the surface plasmon field in terms of linear superpositions of modes having the structure $\exp[i(K_x x + K_y y + \gamma z - \omega t)]$ with a well-defined polarization. Each representation is associated with either a complex frequency or a complex wave vector and therefore to a particular dispersion relation. We then show that the most convenient choice depends on

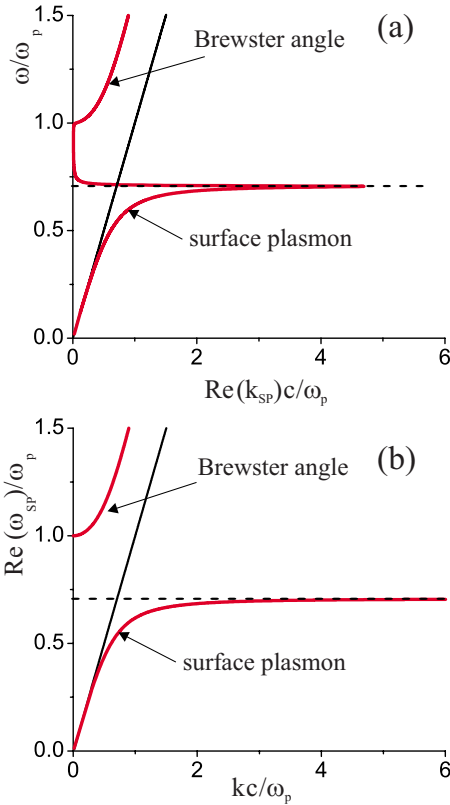


FIG. 1. (Color online) Dispersion of surface plasmons propagating along the metal/air interface. For the sake of illustration, a Drude model is used. (a) Real ω is chosen to obtain a complex K_{sp} . (b) Real K is chosen to obtain a complex ω_{sp} . The flat asymptote (dashed line) situated at $\omega_p/\sqrt{2}$ represents the nonretarded surface plasmon solution. The slanting solid line represents the light cone inside which a wave is propagating (radiative) and outside which is evanescent (surface).

the physical problem to be discussed. We introduce a prescription that allows us to choose complex or real frequency and the associated dispersion relation. We then apply our analysis to discuss the resolution limit issue and the LDOS issue. The paper is organized as follows. For the sake of completeness, we briefly summarize the derivation of the dispersion relation in Sec. II. Section III introduces the general representations of the surface plasmon field. We discuss the physical content of these representations in Sec. IV.

II. SURFACE PLASMON DISPERSION RELATION

Let us consider a flat metal surface $z=0$ bounded by dielectric media with dielectric constant ϵ_1 . We derive the dispersion relation of surface plasmons propagating along the metal/dielectric interface. We seek a solution of Maxwell equations for an interface between two linear isotropic and local media characterized by dielectric constants ϵ_m , where $m=1,2$ denotes medium 1 ($z<0$) or 2 ($z>0$). A surface wave solution has a structure $\exp[i(\mathbf{K}\cdot\mathbf{r} + \gamma_m|z| - \omega t)]$ with

$$\mathbf{K}^2 + \gamma_m^2 = \epsilon_m \omega^2 / c^2, \quad (1)$$

where γ_m is chosen so that $\Im\gamma_m > 0$. Boundary conditions impose the continuity of the tangential components of the

electric field and ϵE_z . It follows that a p -polarized field can exist provided that $\epsilon_1 \gamma_2 = -\epsilon_2 \gamma_1$. One finds that a solution is given by

$$K^2 = \left(\frac{\omega}{c}\right)^2 \frac{\epsilon_1 \epsilon_2}{\epsilon_1 + \epsilon_2}. \quad (2)$$

When dealing with an interface separating a dielectric from a nonlossy metal, $\frac{\epsilon_1 \epsilon_2}{\epsilon_1 + \epsilon_2}$ yields a unique solution to the problem. When accounting for losses in the material, $\frac{\epsilon_1 \epsilon_2}{\epsilon_1 + \epsilon_2}$ is a complex number so that the dispersion relation cannot be solved using real K and real ω . It is necessary to consider a complex frequency or a complex wave vector to find roots of the equation. Let us first choose ω real. We denote K_{sp} the complex root of Eq. (2). Figure 1(a) shows the dispersion curve obtained from the surface plasmon dispersion relation [Eq. (2)] when plotting ω versus $\Re K_{\text{sp}}$. This curve exhibits a backbending in the vicinity of the frequency of nonretarded surface plasmon $\omega_p/\sqrt{2}$. The second possible choice is to keep a real wave vector \mathbf{K} . We denote ω_{sp} the complex root of Eq. (2). For the sake of illustration, we describe the dielectric response of the metal to an electric field using the local Drude model,

$$\epsilon_2(\omega) = 1 - \frac{\omega_p^2}{\omega(\omega + i\nu_e)}, \quad (3)$$

where ω_p is the bulk-plasmon frequency and ν_e is a phenomenological bulk electron relaxation rate. It is worth noting that Drude's model is valid in the IR part of the spectrum for noble metals but fails for frequencies in the interband absorption spectra (at frequencies higher than 3.5 eV for silver and 2.2 for gold). A better model can be found in Refs. 29 and 30. However, Drude's model is convenient for the sake of illustration of the issues discussed in this paper. Figure 1(b) shows the dispersion curve obtained when plotting $\Re \omega_{\text{sp}}$ versus K . It is seen in Fig. 1(b) that this curve exhibits an asymptote for large wave vectors.

Let us make two remarks regarding the dispersion relation. We first note that Eq. (2) is also a solution of $\epsilon_1 \gamma_2 = \epsilon_2 \gamma_1$ which defines a zero of the reflection factor, i.e., the Brewster angle. It can be checked that the upper branch in Fig. 1(b) is not a surface wave but the locus of the Brewster angle in the (ω, K) plane. Finally, we note that a surface plasmon is a collective oscillation of charge density. When the frequency ω is smaller than ν_e , the collective electron oscillation is overdamped. In this low-frequency regime, Eq. (2) describes a surface wave that has been known since the early days of radiowave propagation and called Sommerfeld's surface wave.³¹ Yet, this wave has no longer the character of a surface plasmon. Thus, Eq. (2) describes Brewster angle for $\omega > \omega_p$, a surface plasmon for $\omega_p > \omega > \nu_e$, and a Sommerfeld's surface wave for $\nu_e > \omega$.

III. GENERAL FIELD REPRESENTATIONS

The aim of this section is to derive a general form of the surface plasmon field. To this aim, we first use the simple interface Green's tensor that yields the general form of the

field for any given source distribution. We then extract the surface plasmon contribution which is defined to be the pole contribution to the Green's tensor. We will show that this procedure leads in a natural way to different representations that make use of either a complex wave vector or a complex frequency. We emphasize that both representations will describe the same electromagnetic surface plasmon field $\mathbf{E}_{\text{sp}}(x, y, z, t)$.

Let us suppose that an arbitrary source is located nearby the dielectric-metal interface. The electric field generated by the source current density $\mathbf{j}(\mathbf{r}, t)$ is given by the relation

$$\mathbf{E}(\mathbf{r}, t) = -\mu_0 \int dt' \int d^3\mathbf{r}' \vec{G}(\mathbf{r}, \mathbf{r}', t-t') \frac{\partial \mathbf{j}(\mathbf{r}', t')}{\partial t'}, \quad (4)$$

where μ_0 is vacuum permeability. A Fourier representation can be written in the form

$$\vec{G}(\mathbf{r}, \mathbf{r}', t-t') = \int \frac{d^2\mathbf{K}}{4\pi^2} \int \frac{d\omega}{2\pi} \vec{g}(\mathbf{K}, z, z', \omega) e^{i[\mathbf{K}(\mathbf{r}-\mathbf{r}')-\omega(t-t')]}. \quad (5)$$

Here, the integration variables K_x, K_y and ω are real. The explicit form of the Green's tensor $\vec{g}(\mathbf{K}, z, z', \omega)$ in the presence of the interface is given in Appendix A. It is seen that the Fourier transform of the Green's tensor has poles given by the denominator of the Fresnel factors for p -polarized field. For a dielectric/metal interface, they correspond to the surface plasmon as discussed previously. Thus, the Green's tensor can be split into two terms: the pole contribution that yields the surface plasmon and the remaining contribution that yields a regularized Green's tensor,

$$\vec{G} = \vec{G}_{\text{reg}} + \vec{G}_{\text{sp}}, \quad (6)$$

where the pole contribution to the Green's tensor \vec{G}_{sp} can be explicitly derived using the residue theorem. \vec{G}_{reg} is the contribution of the regularized Green's dyadic. It can be shown that the Green's tensor can be evaluated using a contour deformation in the complex plane and that the regularized term is essentially due to the contribution along the branch cut. This contribution is often termed cylindrical wave or creeping wave. The relative importance of these terms is well documented in classical texts for radiowaves.^{31,32} The analysis of their respective contribution was of practical importance in the early days of telecommunications as radiowaves were guided by the earth. This issue has been discussed recently in the context of optics.^{4,33} In this paper, we shall not pursue this discussion and focus instead on the surface wave contribution defined as the pole contribution,

$$\mathbf{E}_{\text{sp}}(\mathbf{r}, t) = -\mu_0 \int dt' \int d^3\mathbf{r}' \vec{G}_{\text{sp}}(\mathbf{r}, \mathbf{r}', t-t') \frac{\partial \mathbf{j}(\mathbf{r}', t')}{\partial t'}. \quad (7)$$

When solving Eq. (2), we can consider that ω is real and find a complex K_{sp} or we can impose a real value to K and find a complex root ω_{sp} . Thus, when extracting the poles, it is a matter of choice to consider that they are poles in the complex-frequency plane or in the complex wave-vector plane. We find either a couple of poles ω_{sp} and $-\omega_{\text{sp}}^*$ or a complex wave-vector pole K_{sp}^2 . Thus there are two poles for

the component of the wave vector along the x axis, $K_{x,\text{sp}}$ and $-K_{x,\text{sp}}$, for a given component along the y axis K_y as $K_{\text{sp}}^2 = K_{x,\text{sp}}^2 + K_y^2$. It follows that we can cast the pole contribution to the Green's tensor in the form

$$\vec{g}_{\text{sp}}(\mathbf{K}, z, z', \omega) = \frac{\vec{f}_{\omega_{\text{sp}}}(\mathbf{K}, z, z')}{\omega - \omega_{\text{sp}}} + \frac{\vec{f}_{-\omega_{\text{sp}}^*}(\mathbf{K}, z, z')}{\omega + \omega_{\text{sp}}^*}, \quad (8)$$

where $\vec{f}_{\omega_{\text{sp}}}(\mathbf{K}, z, z')$ and $\vec{f}_{-\omega_{\text{sp}}^*}(\mathbf{K}, z, z')$ are the residues of \vec{g} at ω_{sp} and $-\omega_{\text{sp}}^*$, respectively, or in the form

$$\vec{g}_{\text{sp}}(\mathbf{K}, z, z', \omega) = \frac{\vec{f}_{K_{x,\text{sp}}}(K_y, z, z', \omega)}{K_x - K_{x,\text{sp}}} + \frac{\vec{f}_{-K_{x,\text{sp}}}(K_y, z, z', \omega)}{K_x + K_{x,\text{sp}}},$$

where $\vec{f}_{K_{x,\text{sp}}}(K_y, z, z', \omega)$ and $\vec{f}_{-K_{x,\text{sp}}}(K_y, z, z', \omega)$ are the residues of \vec{g} at $K_{x,\text{sp}}$ and $-K_{x,\text{sp}}$, respectively. These two choices lead to two different forms of the surface plasmon field given by Eq. (7). We now examine these forms in detail.

A. Surface plasmon field representation with a real wave vector

In this section we derive the analytical form of the surface plasmon field using real wave vectors. For this purpose we evaluate the pole contribution to the Green's tensor by integrating in the complex ω plane. The complex pole ω_{sp} then yields a contribution for $t-t' > 0$ that varies as $\exp[-i\omega_{\text{sp}}(t-t')]$. After integration, we find

$$\vec{G}_{\text{sp}} = H(t-t') 2\Re \int \frac{d^2\mathbf{K}}{(2\pi)^2} (-i) \vec{f}_{\omega_{\text{sp}}}(\mathbf{K}, z, z') \times e^{i[\mathbf{K}(\mathbf{r}-\mathbf{r}')-\omega_{\text{sp}}(t-t')]}, \quad (9)$$

where $\vec{f}_{\omega_{\text{sp}}}(\mathbf{K}, z, z')$ is the residue of \vec{g} at ω_{sp} . It is given in Appendix A. It follows from Eq. (7) that the field can be cast in the form of a linear superposition of modes with real wave vector and complex frequency,

$$\mathbf{E}_{\text{sp}} = 2\Re \int \frac{d^2\mathbf{K}}{(2\pi)^2} E(\mathbf{K}, t) \left(\hat{\mathbf{K}} - \frac{K}{\gamma_m} \mathbf{n}_m \right) e^{i(\mathbf{K}\cdot\mathbf{r} + \gamma_m |z| - \omega_{\text{sp}} t)}, \quad (10)$$

where we have used the notations $\mathbf{n}_m = -\hat{\mathbf{z}}$ if $z < 0$ and $\hat{\mathbf{z}}$ if $z > 0$, $\hat{\mathbf{K}} = \mathbf{K}/K$, and the amplitude $E(\mathbf{K}, t)$ is given in Appendix A. Note that the polarization of each mode is specified by the complex vector $\hat{\mathbf{K}} - \frac{K}{\gamma_m} \mathbf{n}_m$, whose component along the z axis depends on the medium from which the field is evaluated.

The surface plasmon field takes a form that looks as a mode superposition *except that the amplitude $E(\mathbf{K}, t)$ depends on the time t* . Indeed, when describing a stationary field using modes that have an exponential decay, the amplitude is necessarily time dependent. Note also that sources must be active in order to compensate for the losses in order to maintain a stationary regime. If we consider a situation where the sources are extinguished after time $t=0$, the amplitude $E(\mathbf{K}, t)$ becomes time independent. The time decay of the mode is well described by the imaginary part of ω_{sp} . The representation with complex frequencies given by Eq. (10) is

thus well suited to describe the free evolution of the field once the sources are turned off. It is typically well suited to analyze the fields produced by short pulses.

B. Surface plasmon field representation with a real frequency

Let us now turn to the alternative choice. We consider the complex poles $K_{x,\text{sp}}$ and $-K_{x,\text{sp}}$. The Green's function can be cast in the form

$$\begin{aligned} \vec{G}_{\text{sp}} = & i \int \frac{d\omega}{2\pi} \int \frac{dK_y}{2\pi} \vec{f}_{K_{x,\text{sp}}} (K_y, z, z', \omega) e^{iK_{x,\text{sp}}(x-x')} \\ & \times e^{iK_y(y-y')} e^{-i\omega(t-t')} \end{aligned} \quad (11)$$

if $x-x' > 0$ and

$$\begin{aligned} \vec{G}_{\text{sp}} = & -i \int \frac{d\omega}{2\pi} \int \frac{dK_y}{2\pi} \vec{f}_{-K_{x,\text{sp}}} (K_y, z, z', \omega) e^{-iK_{x,\text{sp}}(x-x')} \\ & \times e^{iK_y(y-y')} e^{-i\omega(t-t')} \end{aligned} \quad (12)$$

if $x-x' < 0$. $\vec{f}_{K_{x,\text{sp}}}(K_y, z, z', \omega)$ and $\vec{f}_{-K_{x,\text{sp}}}(K_y, z, z', \omega)$ are the residues of \vec{g} at $K_{x,\text{sp}}$ and $-K_{x,\text{sp}}$. They are given in Appendix A. Inserting Eqs. (11) and (12) in Eq. (7), we obtain the field in the form

$$\begin{aligned} \mathbf{E} = & \int \frac{d\omega}{2\pi} \int \frac{dK_y}{2\pi} \left[E_{>}(K_y, \omega, x) \right. \\ & \times \left(\hat{\mathbf{K}}^+ - \frac{K_{\text{sp}}}{\gamma_m} \mathbf{n}_m \right) e^{i(K_{x,\text{sp}}x + K_y y + \gamma_m |z| - \omega t)} + E_{<}(K_y, \omega, x) \\ & \left. \times \left(\hat{\mathbf{K}}^- - \frac{K_{\text{sp}}}{\gamma_m} \mathbf{n}_m \right) e^{i(-K_{x,\text{sp}}x + K_y y + \gamma_m |z| - \omega t)} \right], \end{aligned} \quad (13)$$

where $\hat{\mathbf{K}}^+ = (K_{x,\text{sp}}\hat{\mathbf{x}} + K_y\hat{\mathbf{y}})/K_{\text{sp}}$ and $\hat{\mathbf{K}}^- = (-K_{x,\text{sp}}\hat{\mathbf{x}} + K_y\hat{\mathbf{y}})/K_{\text{sp}}$. The amplitudes $E_{>}(K_y, \omega, x)$ and $E_{<}(K_y, \omega, x)$ are given in Appendix A. It is seen that they depend on the position x . Equation (13) can be simplified if we consider that all sources lie in the $x < 0$ region and the region of interest is the $x > 0$ region. Then in a source-free region $E_{>}(K_y, \omega, x)$ does not depend anymore on x according to Eq. (A12) and $E_{<}(K_y, \omega, x)$ equals to zero according to Eq. (A13) as no source lies in the $x' > x$ region. The surface plasmon field can then be cast in the form

$$\mathbf{E} = \int \frac{d\omega}{2\pi} \int \frac{dK_y}{2\pi} \left(\hat{\mathbf{K}} - \frac{K_{\text{sp}}}{\gamma_m} \mathbf{n}_m \right) E_{>}(K_y, \omega) e^{i(\mathbf{K}\cdot\mathbf{r} + \gamma_m |z| - \omega t)}, \quad (14)$$

where $\mathbf{K} = K_{x,\text{sp}}\hat{\mathbf{x}} + K_y\hat{\mathbf{y}}$, $K_{x,\text{sp}} = (K_{\text{sp}}^2 - K_y^2)^{1/2}$ with $\Im m(K_{x,\text{sp}}) \geq 0$ and $\Re e(K_{x,\text{sp}}) \geq 0$, and $\hat{\mathbf{K}} = \mathbf{K}/K_{\text{sp}}$. We conclude that stationary monochromatic fields propagating in a source-free region are well described by a representation that uses complex wave vectors and real frequencies. This equation is one of the main results of this paper. Indeed, it provides a rigorous framework that can be used to develop surface plasmon Fourier optics. Similar representations have been postulated as ansatz in the literature in order to deal with surface plasmons interferences,²⁶ propagation along a stripe,⁵ or

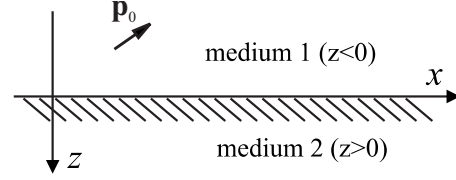


FIG. 2. A pointlike dipole located nearby the dielectric-metal interface.

focusing.²⁵ The framework introduced above provides a rigorous vectorial form of the surface plasmon field valid in a source-free region. Let us emphasize that this representation is well suited to discuss propagation for $x > x_0$ of a surface plasmon field known along a line $x = x_0$. It is seen on Eq. (14) that propagation over a distance d amounts to multiply each mode by a factor $\exp(iK_x d)$. In general, this involves modifying both the phase and the amplitude of the mode. Thus, it allows to discuss any surface wave diffraction problem. Finally, let us stress that this representation is valid for a complex wave vector \mathbf{K} and a real frequency ω so that this representation is necessarily associated with a dispersion relation with backbending.

To summarize, we have shown that the surface plasmon field can be represented using modes that have either a complex frequency or a complex wave vector. If there are active sources, the amplitudes still depend on either time or space. In the case of a field excited by a pulse, the representation that uses complex frequencies is well suited after the pulse. It is associated with the dispersion relation without backbending. In the case of a stationary monochromatic excitation localized in space, a representation using modes with complex wave vectors is well suited outside the excitation region. It corresponds to a dispersion relation with backbending. This simple analysis yields a simple prescription to choose the more suitable representation and the corresponding dispersion relation. Note that in the case of pulses limited in space both representations can be used.

C. Surface plasmon field generated by a dipole

For many applications, it is useful to know the field generated by a dipole. For instance, when considering the field scattered by a subwavelength particle, the source can be represented by an electric dipole. In addition, any source can be decomposed as linear superposition of dipolar sources. Here, we derive the surface plasmon field generated by a monochromatic pointlike dipole characterized by its dipole moment \mathbf{p}_0 (see Fig. 2). Note that there are other contributions to the field generated by the dipole at a distance typically smaller than a wavelength. The surface plasmon contribution is typically dominant for larger distances.^{33,34}

For a vertical dipole $\mathbf{p}_0 e^{-i\omega_0 t} = p_0 e^{-i\omega_0 t} \hat{\mathbf{z}}$ located at a distance d below the interface, at $x = y = 0$, we obtain, using the cylindrical basis $(\hat{\rho}, \hat{\theta}, \hat{\mathbf{z}})$

$$\begin{aligned} \mathbf{E}_m = & 2\Re e \left\{ \left[H_1^{(1)}(K_{\text{sp}}\rho) \hat{\rho} + i \frac{K_{\text{sp}}}{\gamma_m} H_0^{(1)}(K_{\text{sp}}\rho) \mathbf{n}_m \right] \right. \\ & \left. \times M(K_{\text{sp}}, \omega_0) \frac{1}{\epsilon_0} (-i) \frac{K_{\text{sp}}}{\gamma_1} p_0 e^{i\gamma_1 d} e^{i\gamma_m |z|} e^{-i\omega_0 t} \right\}, \end{aligned} \quad (15)$$

where $H_0^{(1)}$ and $H_1^{(1)}$ are the Hankel functions of the first kind

of zeroth and first order, respectively, K_{sp} is complex and satisfies Eq. (2) with $\omega = \omega_0$, $M(K_{\text{sp}}, \omega_0)$ is given in Appendix B and the other notations are defined above. The details of the calculation are given in Appendix B. Using the asymptotic forms of the Hankel functions, we obtain for the field of a vertical dipole, for ρ greater than a few $1/|K_{\text{sp}}|$

$$\mathbf{E}_m = 2\Re\epsilon \left[\frac{e^{iK_{\text{sp}}\rho}}{\sqrt{K_{\text{sp}}\rho}} \left(\hat{\rho} - \frac{K_{\text{sp}}}{\gamma_m} \mathbf{n}_m \right) \times M'_v(K_{\text{sp}}, \omega_0) p_0 e^{i\gamma_1 d} e^{i\gamma_m |z|} e^{-i\omega_0 t} \right], \quad (16)$$

where $M'_v(K_{\text{sp}}, \omega_0)$ is given in Appendix B. Thus the surface plasmon field is analogous to a damped cylindrical wave $\frac{e^{iK_{\text{sp}}\rho}}{\sqrt{K_{\text{sp}}\rho}}$ with a polarization vector $\hat{\rho} - \frac{K_{\text{sp}}}{\gamma_m} \mathbf{n}_m$. For a dipole oriented along the x axis $\mathbf{p}_0 e^{-i\omega_0 t} = p_0 e^{-i\omega_0 t} \hat{\mathbf{x}}$, we obtain

$$\mathbf{E}_m = 2\Re\epsilon \left\{ \left[\left[H_1^{(1)}(K_{\text{sp}}\rho) \right]' \hat{\rho} - i \frac{K_{\text{sp}}}{\gamma_m} H_1^{(1)}(K_{\text{sp}}\rho) \mathbf{n}_m \right] \times \cos \theta - \frac{H_1^{(1)}(K_{\text{sp}}\rho)}{K_{\text{sp}}\rho} \hat{\theta} \sin \theta \right] \times M(K_{\text{sp}}, \omega_0) \frac{1}{\epsilon_0} p_0 e^{i\gamma_1 d} e^{i\gamma_m |z|} e^{-i\omega_0 t} \right\}, \quad (17)$$

where $\theta = (\hat{\mathbf{x}}, \hat{\rho})$. Using the asymptotic forms of the Hankel functions, we obtain

$$\mathbf{E}_m = 2\Re\epsilon \left[\frac{e^{iK_{\text{sp}}\rho}}{\sqrt{K_{\text{sp}}\rho}} \left(\hat{\rho} - \frac{K_{\text{sp}}}{\gamma_m} \mathbf{n}_m \right) \times \cos \theta M'_h(K_{\text{sp}}, \omega_0) p_0 e^{i\gamma_1 d} e^{i\gamma_m |z|} e^{-i\omega_0 t} \right], \quad (18)$$

where $M'_h(K_{\text{sp}}, \omega_0)$ is given in Appendix B. Here we have neglected the terms decreasing faster than $1/\sqrt{\rho}$, thus Eq. (18) gives the surface plasmon amplitude in the far-field regime where the asymptotic representation of the Hankel function can be applied. The asymptotic surface plasmon field is analogous to a damped cylindrical wave $\frac{e^{iK_{\text{sp}}\rho}}{\sqrt{K_{\text{sp}}\rho}}$ with the same polarization vector $\hat{\rho} - \frac{K_{\text{sp}}}{\gamma_m} \mathbf{n}_m$ times a factor $\cos \theta$. The later makes the far field vanishing in the direction perpendicular to the dipole (here the y direction) and more intense in the dipole direction (here the x direction). Note that the y component of the surface plasmon field vanishes only in the far-field regime, while its contribution remains significant in the near field.

IV. DISCUSSION

In this section, we revisit two fundamental issues in the field of surface plasmons: field confinement and large density of states. Confinement and super-resolution are related to the existence of wave vectors with a modulus much larger than ω/c . In this respect the choice of the proper dispersion relation plays a key role as one has a cut-off wave vector, whereas the other predicts no limit for the dispersion relation. Is there a limit to the resolution? Is there a limit to the local density of states?

A. Super-resolution

Let us first discuss the issue of resolution when imaging with a surface plasmon driven at frequency ω by an external source. Recent experiments on far-field optical microscopy¹⁹ initiated a debate^{35,36} about the role of surface plasmons in super-resolution imaging effects. In Ref. 19 the dispersion curve with the asymptotic behavior has been invoked to stress the role of surface plasmons in the image formation with nanoresolution. The resolution was estimated to be $\lambda_{\text{sp}}/2$. Therefore, if the dispersion curve with the asymptotic behavior is chosen, there seems to be no diffraction limit and only the amplitude decay of surface plasmon due to Ohmic losses in the metal limits the resolution. The effect of the backbending of surface plasmon dispersion discussed in Ref. 36 limits the surface plasmon wavelength $2\pi/\Re K_{\text{sp}}$ and therefore, the resolution. Clearly, both dispersion relations do not lead to the same conclusion and a prescription to choose one or the other is needed. Let us consider a situation where a surface plasmon is excited locally by a stationary monochromatic field. From Sec. III, we know that a representation with fixed amplitudes using modes with complex wave vectors and real frequencies is valid outside the source region. This implies that the dispersion relation with real frequency (with backbending) is relevant. It follows that there is a cut-off spatial frequency. Indeed, as K_x may be complex, the propagation term $\exp(iK_x x)$ introduces damping. In the case of a lossy medium, damping may be due to losses. However, even for a nonlossy medium (K_{sp} is real), $K_x = (K_{\text{sp}}^2 - K_y^2)^{1/2}$ can be imaginary. This occurs when K_y exceeds the value K_{sp} . This situation is the two-dimensional (2D) analog of the evanescent waves with wave vector K larger than ω/c that cannot propagate in a vacuum. Clearly, K_{sp} is a cut-off frequency and the propagation term $\exp(iK_x x)$ works as a low-pass filter that prevents propagation of fields associated with spatial frequencies k_y larger than K_{sp} . When dealing with lossy media, it is the real part of K_{sp} that specifies the cut-off spatial frequency. It is seen in Fig. 1 that K_{sp} has a maximum value at the backbending of the dispersion relation.

In summary, when discussing imaging using stationary monochromatic surface plasmons, the relevant representation is based on modes with a complex wave vector and a real frequency given by Eq. (14). This corresponds to a dispersion relation that has a backbending. It follows that the resolution is limited by the cut-off spatial frequency given by the maximum value of $\Re K_{\text{sp}}$.

B. Local density of states

Let us now discuss the LDOS. The DOS is a quantity that plays a fundamental role in many domains. In particular, it allows to derive all thermodynamic properties of a system. In the case of an interface, the surface modes are confined close to the interface so that it is useful to introduce the LDOS that depends on the distance to the interface.^{37,38} It allows to account for the huge increase in energy density close to an interface when surface waves are excited.^{38,39} It also plays a key role in defining the lifetime of a single emitter close to an interface.⁴⁰⁻⁴⁴ In this context, the increase in the projected LDOS is usually normalized by the LDOS in a homogeneous

medium (e.g., a vacuum) yielding the so-called Purcell factor. It is well known in solid-state physics that the density of states can be derived from the dispersion relation. More specifically, the dispersion relation is proportional to $1/|\nabla_k\omega(k)|$ so that it takes large values when the dispersion relation is flat.

A quick look at Fig. 1 shows that different dispersion relations seem to predict different LDOS. Although the Drude model is not correct for noble metals close to the plasma frequency, it is useful for the sake of illustration. While Fig. 1(b) predicts a very large peak at $\omega_{sp}/\sqrt{2}$ due to the asymptote, Fig. 1(a) predicts a smaller peak and a non-zero LDOS between $\omega_{sp}/\sqrt{2}$ and ω_{sp} . Again, we see that a prescription is needed to choose the right dispersion relation.

A standard procedure to derive the DOS in the reciprocal space is based on the introduction of discrete modes using periodic boundary conditions. Assuming a surface of side L , the wave vector takes the form $\mathbf{K}=n_x\frac{2\pi}{L}\hat{\mathbf{x}}+n_y\frac{2\pi}{L}\hat{\mathbf{y}}$. In the plane K_x, K_y , a mode has an area $4\pi^2/L^2$. It follows that the number of modes per unit area in $d^2\mathbf{K}$ is given by $d^2\mathbf{K}/4\pi^2$. When performing this analysis, both K_x and K_y are real. Thus the relevant representation uses real wave vectors and complex frequencies. The corresponding dispersion relation has no backbending and therefore presents a singularity. This is in agreement with another approach of the LDOS based on the use of the Green's tensor that predicts an asymptotic behavior proportional to $1/(z^3|\epsilon+1|^2)$.^{37,38} Of course, this divergence is nonphysical. It is related to the modeling of the medium using a continuous description of the metal. This model cannot be valid on an atomic scale. Before reaching the atomic scale, nonlocal effects must be taken into account.

V. CONCLUSION

In this work we have addressed several issues regarding surface plasmons on flat surfaces. The first issue deals with a mode representation of the surface plasmon field. We have shown that a surface plasmon field can be represented as a sum of modes with either a complex wave vector or a complex frequency. We have shown that a representation using complex frequencies is well adapted to fields excited by pulses, i.e., after extinction of the sources. A representation using complex wave vectors is well adapted to stationary monochromatic fields in a source-free region, i.e., beyond the source region. The latter provides a rigorous formula that can be used to analyze the diffraction of a stationary surface plasmon field. This should be very useful in order to develop a surface plasmon Fourier optics framework. This formula clearly shows that the maximum value of $\Re K_{sp}$ is a cut-off spatial frequency that gives an upper limit to the resolution or confinement that can be obtained using surface plasmons. As a by-product, we have derived the form of the surface plasmon excited by a dipole located below the interface. Finally, we have discussed how to choose the dispersion relation (with or without backbending) depending on the issue. To illustrate this procedure, we have shown that there is a resolution limit given by the maximum value of the wave vector at the backbending point. We have also shown that the local density of states should be analyzed using the disper-

sion relation with a real wave vector. This yields a LDOS that diverges close to the interface in agreement with the result obtained from the Green's tensor approach.

ACKNOWLEDGMENTS

This work was supported by the French National Research Agency (ANR) through Carnot Leti funding and by the French Ministry of Defense through a grant from the *Direction g n rale de l'armement* (DGA).

APPENDIX A: CALCULATIONS OF THE SURFACE PLASMON FIELD

For the plane interface system, it is convenient to use the representation introduced by Sipe⁴⁵ that consists of a decomposition over elementary plane waves. We consider the interface separating medium 1 ($z < 0$) from medium 2 ($z > 0$). We use the dyadic notation for the tensors. For instance, the s component of the electric field is given by $\hat{s}\hat{s}\mathbf{E}=\hat{s}(\hat{s}\cdot\mathbf{E})$. Using the notations of Eq. (5), the Green's tensor can be cast in the form ($z, z' < 0$)

$$\vec{g}(\mathbf{K}, z, z', \omega) = \vec{g}_0(\mathbf{K}, z, z', \omega) + \frac{i}{2\gamma_1} [\hat{s}r_s\hat{s} + \hat{p}_1^- r_p \hat{p}_1^+] e^{-i\gamma_1 z'} e^{-i\gamma_1 z}, \quad (\text{A1})$$

where $\vec{g}_0(\mathbf{K}, z, z', \omega)$ denotes the Fourier transform of the Green's tensor in a homogeneous medium 1.

The Green's tensor for ($z > 0$) and ($z' < 0$) can be written in the form

$$\vec{g}(\mathbf{K}, z, z', \omega) = \frac{i}{2\gamma_1} [\hat{s}t_s\hat{s} + \hat{p}_2 t_p \hat{p}_1^+] e^{-i\gamma_1 z'} e^{i\gamma_2 z}. \quad (\text{A2})$$

The Fresnel reflection and transmission factors are given by

$$r_s = \frac{\gamma_1 - \gamma_2}{\gamma_1 + \gamma_2} \quad r_p = \frac{\gamma_1 \epsilon_2 - \gamma_2 \epsilon_1}{\gamma_1 \epsilon_2 + \gamma_2 \epsilon_1}, \quad (\text{A3})$$

$$t_s = \frac{2\gamma_1}{\gamma_1 + \gamma_2} \quad t_p = \frac{2\gamma_1 \sqrt{\epsilon_1} \sqrt{\epsilon_2}}{\gamma_1 \epsilon_2 + \gamma_2 \epsilon_1}, \quad (\text{A4})$$

where $\gamma_m = \sqrt{\epsilon_m(\frac{\omega}{c})^2 - K^2}$ is chosen so that $\Im m \gamma_m > 0$. Using $\epsilon_m(-\omega^*) = \epsilon_m^*(\omega)$, we obtain $\gamma_m(K^*, -\omega^*) = -\gamma_m^*(K, \omega)$. The square roots of dielectric constants $\sqrt{\epsilon_m}$ are chosen so that $\Re \epsilon_m \geq 0$. We now introduce the s and p polarization vectors $\hat{s} = \mathbf{K} \times \mathbf{z}/K$, $\hat{p}_1^\pm = (Kz \mp \gamma_1 \mathbf{K}/K)/(k_0 \sqrt{\epsilon_1})$, and $\hat{p}_2 = (Kz - \gamma_2 \mathbf{K}/K)/(k_0 \sqrt{\epsilon_2})$, and the notation $k_0 = \omega/c$. $K = \sqrt{K_x^2 + K_y^2}$ is chosen so that $\Im m K > 0$ or $\Im m K = 0$ and $\Re \epsilon K > 0$. It follows that $\hat{p}(-\mathbf{K}, -\omega^*) = -\hat{p}(\mathbf{K}, \omega)^*$ when \mathbf{K} is real and ω complex and $\hat{p}(-\mathbf{K}^*, -\omega) = \hat{p}(\mathbf{K}, \omega)^*$ when \mathbf{K} is complex and ω real.

We extend the definition of $\vec{g}(\mathbf{K}, z, z', \omega)$ to complex values of ω and assume that the denominator of the Fresnel coefficients r_p and t_p [whose nullity is equivalent to Eq. (2)] has two roots ω_{sp} and $-\omega_{sp}^*$.

$$\frac{1}{\gamma_1 \epsilon_2 + \gamma_2 \epsilon_1} = \frac{C(K, \omega)}{(\omega - \omega_{\text{sp}})(\omega + \omega_{\text{sp}})}, \quad (\text{A5})$$

with $\Im \omega_{\text{sp}} < 0$. The residues of \vec{g} at these poles can be calculated with $\vec{f}_{\tilde{\omega}}(\mathbf{K}, z, z') = \lim_{\omega \rightarrow \tilde{\omega}} [(\omega - \tilde{\omega}) \vec{g}(\mathbf{K}, z, z', \omega)]$, where $\tilde{\omega}$ denotes ω_{sp} or $-\omega_{\text{sp}}^*$. We find

$$\vec{f}_{\omega_{\text{sp}}}(\mathbf{K}, z, z') = i \frac{\gamma_1 \epsilon_2}{k_0 \sqrt{\epsilon_1}} \frac{C(K, \omega_{\text{sp}})}{2\Re \omega_{\text{sp}}} \left(\hat{\mathbf{K}} - \frac{K}{\gamma_m} \mathbf{n}_m \right) \hat{\mathbf{p}}_1^+ e^{-i\gamma_1 z'} e^{i\gamma_m |z|}, \quad (\text{A6})$$

where \mathbf{n}_m denotes $-\hat{\mathbf{z}}$ for $z < 0$ and $\hat{\mathbf{z}}$ for $z > 0$ and γ_m denotes γ_1 for $z < 0$ and γ_2 for $z > 0$. γ_1 and γ_2 depends on K and ω_{sp} and $\hat{\mathbf{p}}_1^+$ depends on \mathbf{K} and ω_{sp} .

Using $\epsilon_m(-\omega^*) = \epsilon_m^*(\omega)$, $\gamma_m(K, -\omega^*) = -\gamma_m^*(K, \omega)$, and $\hat{\mathbf{p}}_1^+(\mathbf{K}, -\omega^*) = -\hat{\mathbf{p}}_1^+(\mathbf{K}, \omega)^*$, we have

$$\vec{f}_{-\omega_{\text{sp}}^*}(\mathbf{K}, z, z') = -\vec{f}_{\omega_{\text{sp}}}^*(\mathbf{K}, z, z'). \quad (\text{A7})$$

Using Eqs. (7), (9), and (A6), we find the amplitudes in Eq. (10):

$$E(\mathbf{K}, t) = -\mu_0 \frac{\gamma_1 \epsilon_2}{k_0 \sqrt{\epsilon_1}} \frac{C(K, \omega_{\text{sp}})}{2\Re \omega_{\text{sp}}} \int d^2 \mathbf{r}' e^{-i\mathbf{K} \cdot \mathbf{r}'} \times \int_{-\infty}^0 dz' e^{-i\gamma_1 z'} \int_{-\infty}^t dt' e^{i\omega_{\text{sp}} t'} \hat{\mathbf{p}}_1^+ \cdot \frac{\partial \mathbf{j}}{\partial t'}(\mathbf{r}', t'). \quad (\text{A8})$$

We now extend the definition of $\vec{g}(\mathbf{K}, z, z', \omega)$ to complex values of K_x and assume that the denominator of the Fresnel

coefficients r_p and t_p has two roots $K_{x,\text{sp}} = \sqrt{K_{\text{sp}}^2 - K_y^2}$ and $-K_{x,\text{sp}}$:

$$\frac{1}{\gamma_1 \epsilon_2 + \gamma_2 \epsilon_1} = \frac{\gamma_1 \epsilon_2 - \gamma_2 \epsilon_1}{\epsilon_1^2 - \epsilon_2^2} \frac{1}{(K_x - K_{x,\text{sp}})(K_x + K_{x,\text{sp}})}, \quad (\text{A9})$$

with $\Im m K_{x,\text{sp}} > 0$ and where K_{sp} depends on ω and is given by the dispersion relation.

The residues of \vec{g} at these poles can be calculated with $\vec{f}_{\tilde{K}_x}(K_y, z, z', \omega) = \lim_{K_x \rightarrow \tilde{K}_x} [(K_x - \tilde{K}_x) \vec{g}(\mathbf{K}, z, z', \omega)]$, where \tilde{K}_x denotes $K_{x,\text{sp}}$ or $-K_{x,\text{sp}}$. We find

$$\vec{f}_{K_{x,\text{sp}}}(K_y, z, z', \omega) = \frac{i}{2K_{x,\text{sp}} k_0 \sqrt{\epsilon_1}} \frac{\gamma_1 \epsilon_2}{\epsilon_1^2 - \epsilon_2^2} \frac{\gamma_1 \epsilon_2 - \gamma_2 \epsilon_1}{\epsilon_1^2 - \epsilon_2^2} \left(\hat{\mathbf{K}}^+ - \frac{K}{\gamma_m} \mathbf{n}_m \right) \hat{\mathbf{p}}_1^+ \times (K_{x,\text{sp}} \hat{\mathbf{x}} + K_y \hat{\mathbf{y}}) e^{-i\gamma_1 z'} e^{i\gamma_m |z|}, \quad (\text{A10})$$

$$\vec{f}_{-K_{x,\text{sp}}}(K_y, z, z', \omega) = -\frac{i}{2K_{x,\text{sp}} k_0 \sqrt{\epsilon_1}} \frac{\gamma_1 \epsilon_2}{\epsilon_1^2 - \epsilon_2^2} \frac{\gamma_1 \epsilon_2 - \gamma_2 \epsilon_1}{\epsilon_1^2 - \epsilon_2^2} \left(\hat{\mathbf{K}}^- - \frac{K}{\gamma_m} \mathbf{n}_m \right) \hat{\mathbf{p}}_1^+ \times (-K_{x,\text{sp}} \hat{\mathbf{x}} + K_y \hat{\mathbf{y}}) e^{-i\gamma_1 z'} e^{i\gamma_m |z|}, \quad (\text{A11})$$

where $\hat{\mathbf{K}}^+ = \frac{K_{x,\text{sp}} \hat{\mathbf{x}} + K_y \hat{\mathbf{y}}}{K_{\text{sp}}}$, $\hat{\mathbf{K}}^- = \frac{-K_{x,\text{sp}} \hat{\mathbf{x}} + K_y \hat{\mathbf{y}}}{K_{\text{sp}}}$, and the other notations are defined above.

Using Eqs. (7), (11), (12), (A10), and (A11), we obtain the amplitudes of the modes in Eq. (13):

$$E_{>}(K_y, \omega, x) = \mu_0 \frac{1}{2K_{x,\text{sp}} k_0 \sqrt{\epsilon_1}} \frac{\gamma_1 \epsilon_2}{\epsilon_1^2 - \epsilon_2^2} \frac{\gamma_1 \epsilon_2 - \gamma_2 \epsilon_1}{\epsilon_1^2 - \epsilon_2^2} \int_{-\infty}^x dx' e^{-iK_{x,\text{sp}} x'} \int dy' e^{-iK_y y'} \int_{-\infty}^0 dz' e^{-i\gamma_1 z'} \int dt' e^{i\omega t'} \hat{\mathbf{p}}_1^+(K_{x,\text{sp}} \hat{\mathbf{x}} + K_y \hat{\mathbf{y}}, \omega) \cdot \frac{\partial \mathbf{j}}{\partial t'}(\mathbf{r}', t'), \quad (\text{A12})$$

$$E_{<}(K_y, \omega, x) = \mu_0 \frac{1}{2K_{x,\text{sp}} k_0 \sqrt{\epsilon_1}} \frac{\gamma_1 \epsilon_2}{\epsilon_1^2 - \epsilon_2^2} \frac{\gamma_1 \epsilon_2 - \gamma_2 \epsilon_1}{\epsilon_1^2 - \epsilon_2^2} \int_x^{\infty} dx' e^{-iK_{x,\text{sp}} x'} \int dy' e^{-iK_y y'} \int_{-\infty}^0 dz' e^{-i\gamma_1 z'} \int dt' e^{i\omega t'} \hat{\mathbf{p}}_1^+(-K_{x,\text{sp}} \hat{\mathbf{x}} + K_y \hat{\mathbf{y}}, \omega) \cdot \frac{\partial \mathbf{j}}{\partial t'}(\mathbf{r}', t'). \quad (\text{A13})$$

APPENDIX B: SURFACE PLASMON FIELD OF A DIPOLE

The current density associated with a time-dependent dipole $\mathbf{p}_0 e^{-i\omega_0 t}$ at a distance d above the interface is given by $\mathbf{j}(\mathbf{r}, t) = 2\Re e [e^{-i\omega_0 t} (-i)\omega_0 \mathbf{p}_0] \delta[\mathbf{r} - (-d)\hat{\mathbf{z}}]$. Using the form of the surface plasmon field given by Eq. (14), one can compute the amplitude with this expression and Eq. (A12):

$$E_{>}(K_y, \omega) = -\frac{\gamma_1 \epsilon_2 - \gamma_2 \epsilon_1}{\epsilon_1^2 - \epsilon_2^2} \frac{\gamma_1 \epsilon_2}{k_0 \sqrt{\epsilon_1}} \frac{1}{2K_{x,\text{sp}}} e^{i\gamma_1 d} \mu_0 \omega_0^2 \hat{\mathbf{p}}_1^+ \times [2\pi \delta(\omega - \omega_0) \mathbf{p}_0 + 2\pi \delta(\omega + \omega_0) \mathbf{p}_0^*] \quad (\text{B1})$$

Hence, using Eq. (14) and the properties $K(-\mathbf{K}^*) = -K^*(\mathbf{K})$, $K_{x,\text{sp}}(K_y, -\omega) = -K_{x,\text{sp}}^*(K_y, \omega)$, $\gamma_m(K^*, -\omega) = -\gamma_m^*(K, \omega)$, $\epsilon_m(-\omega) = \epsilon_m^*(\omega)$, and the definition of $\hat{\mathbf{p}}_1^+$, we get

$$\mathbf{E}_m = -\Re e \left[e^{i\gamma_m |z|} e^{-i\omega_0 t} \frac{\gamma_1 \epsilon_2 - \gamma_2 \epsilon_1}{\epsilon_1^2 - \epsilon_2^2} \frac{\gamma_1 \gamma_2}{\epsilon_0} \int \frac{dK_y}{2\pi} \frac{e^{i\mathbf{K} \cdot \mathbf{r}}}{K_{x,\text{sp}}} \times \left(\hat{\mathbf{K}} - \frac{K}{\gamma_m} \hat{\mathbf{n}}_m \right) \left(\hat{\mathbf{K}} - \frac{K}{\gamma_1} \hat{\mathbf{z}} \right) \cdot \mathbf{p}_0 \right]. \quad (\text{B2})$$

By differentiating $\int \frac{dK_y}{2\pi} \frac{e^{i\mathbf{K} \cdot \mathbf{r}}}{K_{x,\text{sp}}} = \frac{1}{2} H_0^{(1)}(K_{\text{sp}} \rho)$ with respect to x or

y we obtain two identities $\int \frac{dK_y}{2\pi} \frac{e^{iK_x r}}{K_{x,sp}} \hat{\mathbf{K}} = \frac{i}{2} H_1^{(1)}(K_{sp}\rho) \hat{\rho}$ and $\int \frac{dK_y}{2\pi} \frac{e^{iK_x r}}{K_{x,sp}} \hat{\mathbf{K}} \hat{\mathbf{K}} = \frac{1}{2} \{ [H_1^{(1)}(K_{sp}\rho)]' \hat{\rho} \hat{\rho} + \frac{H_1^{(1)}(K_{sp}\rho)}{K_{sp}\rho} \hat{\theta} \hat{\theta} \}$. Using these identities and the value of \mathbf{p}_0 , with $M(K, \omega) = -\frac{\gamma_1 \gamma_2}{4} \frac{\gamma_1 \epsilon_2 - \gamma_2 \epsilon_1}{\epsilon_1^2 - \epsilon_2^2}$, we get Eqs. (15) and (17). According to Eq. (14), the field found in Eqs. (15) and (17) apply in the $x > 0$ half space. Using a symmetry argument, we find easily that they also apply in the $x < 0$ half space.

Equations (15) and (17) can then be simplified using the asymptotic form of the Hankel functions $H_n(z) \rightarrow \sqrt{\frac{2}{\pi z}} e^{iz - 1/2\pi i(n+1/2)}$. Denoting $M'_v(K_{sp}, \omega_0) = -\sqrt{\frac{2}{\pi}} e^{-i\pi/4} M(K_{sp}, \omega_0) \frac{K_{sp}}{\gamma_1 \epsilon_0}$, we obtain Eq. (16). Using also the property of the Hankel functions $H_1'(z) = H_0(z) - \frac{1}{z} H_1(z)$ and denoting $M'_h(K_{sp}, \omega_0) = \sqrt{\frac{2}{\pi}} e^{-i\pi/4} M(K_{sp}, \omega_0) \frac{1}{\epsilon_0}$, we obtain Eq. (18).

*On leave from Institute of Radio Engineering and Electronics (Saratov Division), Russian Academy of Sciences, Zelyonaya 38, 410019 Saratov, Russia.

†jean-jacques.greffet@institutoptique.fr

¹R. H. Ritchie, Phys. Rev. **106**, 874 (1957).

²W. L. Barnes, A. Dereux, and T. W. Ebbesen, Nature (London) **424**, 824 (2003).

³T. W. Ebbesen, H. J. Lezec, H. F. Ghaemi, T. Thio, and P. A. Wolff, Nature (London) **391**, 667 (1998).

⁴H. Liu and P. Lalanne, Nature (London) **452**, 728 (2008).

⁵J. C. Weeber, J. R. Krenn, A. Dereux, B. Lamprecht, Y. Lacroute, and J. P. Goujonnet, Phys. Rev. B **64**, 045411 (2001).

⁶S. I. Bozhevolnyi, V. S. Volkov, E. Devaux, J. Y. Laluet, and T. W. Ebbesen, Nature (London) **440**, 508 (2006).

⁷M. Quinten, A. Leitner, J. R. Krenn, and F. R. Ausseneg, Opt. Lett. **23**, 1331 (1998).

⁸S. A. Maier, P. G. Kik, H. A. Atwater, S. Meltzer, E. Harel, B. E. Koel, and A. A. G. Requicha, Nature Mater. **2**, 229 (2003).

⁹P. Andrew and W. L. Barnes, Phys. Rev. B **64**, 125405 (2001).

¹⁰P. Anger, P. Bharadwaj, and L. Novotny, Phys. Rev. Lett. **96**, 113002 (2006).

¹¹S. Kuhn, U. Hakanson, L. Rogobete, and V. Sandoghdar, Phys. Rev. Lett. **97**, 017402 (2006).

¹²H. Rigneault, J. Capoulade, J. Dintinger, J. Wenger, N. Bonod, E. Popov, T. W. Ebbesen, and P. F. Lenne, Phys. Rev. Lett. **95**, 117401 (2005).

¹³J. B. Khurgin, G. Sun, and R. A. Soref, Appl. Phys. Lett. **93**, 021120 (2008).

¹⁴C. E. Talley, J. B. Jackson, C. Oubre, N. K. Grady, C. W. Hollars, S. M. Lane, T. R. Huser, P. Nordlander, and N. J. Halas, Nano Lett. **5**, 1569 (2005).

¹⁵E. Prodan, C. Radloff, N. J. Halas, and P. Nordlander, Science **302**, 419 (2003).

¹⁶K. L. Kelly, E. Coronado, L. L. Zhao, and G. C. Schatz, J. Phys. Chem. B **107**, 668 (2003).

¹⁷Z. Liu, J. M. Steele, W. Srituravanich, Y. Pikus, C. Sun, and X. Zhang, Nano Lett. **5**, 1726 (2005).

¹⁸N. Fang, H. Lee, C. Sun, and X. Zhang, Science **308**, 534 (2005).

¹⁹I. I. Smolyaninov, J. Elliott, A. V. Zayats, and C. C. Davis, Phys. Rev. Lett. **94**, 057401 (2005).

²⁰T. Taubner, D. Korobkin, Y. Urzhunov, G. Shvets, and R. Hillenbrand, Science **313**, 1595 (2006).

²¹T. V. Teperik, F. Garcia de Abajo, A. G. Borisov, M. Abdelsalam, P. N. Bartlett, Y. Sugawara, and J. J. Baumberg, Nat. Photonics **2**, 299 (2008).

²²F. Marquier, K. Joulain, J. P. Mulet, R. Carminati, J. J. Greffet,

and Y. Chen, Phys. Rev. B **69**, 155412 (2004).

²³J. J. Greffet, R. Carminati, K. Joulain, J. P. Mulet, S. Mainguy, and Y. Chen, Nature (London) **416**, 61 (2002).

²⁴M. Laroche, C. Arnold, F. Marquier, R. Carminati, J. J. Greffet, S. Collin, N. Bardou, and J. L. Pelouard, Opt. Lett. **30**, 2623 (2005).

²⁵L. Feng, K. A. Tetz, B. Slutsky, V. Lomakin, and Y. Fainman, Appl. Phys. Lett. **91**, 081101 (2007).

²⁶R. Zia and M. L. Brongersma, Nat. Nanotechnol. **2**, 426 (2007).

²⁷E. T. Arakawa, M. W. Williams, R. N. Hamm, and R. H. Ritchie, Phys. Rev. Lett. **31**, 1127 (1973).

²⁸R. W. Alexander, G. S. Kovener, and R. J. Bell, Phys. Rev. Lett. **32**, 154 (1974).

²⁹F. Hao and P. Nordlander, Chem. Phys. Lett. **446**, 115 (2007).

³⁰A. Vial, A. S. Grimault, D. Macias, D. Barchiesi, and M. L. de la Chapelle, Phys. Rev. B **71**, 085416 (2005).

³¹A. Banos, *Dipole Radiation in the Presence of a Conducting Half-Space* (Pergamon, New York, 1966).

³²L. Felsen and N. Marcuvitz, *Radiation and Scattering of Waves* (IEEE, New York, 1994).

³³P. Lalanne and J. P. Hugonin, Nat. Phys. **2**, 551 (2006).

³⁴F. Pincemin, A. Sentenac, and J. J. Greffet, J. Opt. Soc. Am. A Opt. Image Sci. Vis **11**, 1117 (1994).

³⁵I. I. Smolyaninov, C. C. Davis, J. Elliott, and A. V. Zayats, Phys. Rev. Lett. **98**, 209704 (2007).

³⁶A. Drezet, A. Hohenau, and J. R. Krenn, Phys. Rev. Lett. **98**, 209703 (2007).

³⁷K. Joulain, R. Carminati, J. P. Mulet, and J. J. Greffet, Phys. Rev. B **68**, 245405 (2003).

³⁸K. Joulain, J. P. Mulet, F. Marquier, R. Carminati, and J. J. Greffet, Surf. Sci. Rep. **57**, 59 (2005).

³⁹A. V. Shchegrov, K. Joulain, R. Carminati, and J. J. Greffet, Phys. Rev. Lett. **85**, 1548 (2000).

⁴⁰R. R. Chance, A. Prock, and R. Silbey, Adv. Chem. Phys. **37**, 1 (1978).

⁴¹C. Henkel and K. Joulain, Appl. Phys. B: Lasers Opt. **84**, 61 (2006).

⁴²J. Nelayah, M. Kociak, O. Stephan, F. Garcia de Abajo, M. Tence, L. Henrard, D. Taverna, I. Pastoriza-Santos, L. M. Liz-Marzan, and C. Colliex, Nat. Phys. **3**, 348 (2007).

⁴³F. J. Garcia de Abajo and M. Kociak, Phys. Rev. Lett. **100**, 106804 (2008).

⁴⁴C. Chicanne, T. David, R. Quidant, J. C. Weeber, Y. Lacroute, E. Bourillot, A. Dereux, G. Colas des Francs, and C. Girard, Phys. Rev. Lett. **88**, 097402 (2002).

⁴⁵J. E. Sipe, J. Opt. Soc. Am. B **4**, 481 (1987).